Engineering Notes

ENGINEERING NOTES are short manuscripts describing new developments or important results of a preliminary nature. These Notes cannot exceed 6 manuscript pages and 3 figures; a page of text may be substituted for a figure and vice versa. After informal review by the editors, they may be published within a few months of the date of receipt. Style requirements are the same as for regular contributions (see inside back cover).

Flutter Analysis of the CF-18 Aircraft at Supersonic Speeds

B. H. K. Lee*
National Research Council, Ottawa, Ontario, Canada

Introduction

In recent years, a number of studies[1-3] on supersonic aerodynamics computations have appeared. This is motivated by the need of an efficient method for flutter analysis of high-performance, thin-winged fighter aircraft. These methods are based on the velocity potential gradient formulation and do not suffer from the limitations of the traditional Mach box techniques that were widely used nearly a decade ago.[4,5] A distinct advantage of these new developments is that multiple interfering lifting surface configurations can be modeled without any difficulties and the possibilities of including bodies[6] in the computer code make them extremely attractive. It appears that a supersonic counterpart to the subsonic doublet lattice method[7] will become available in the near future.

At the National Aeronautical Establishment, the method of Burkhart[8] is available for use in flutter analysis. In a recent update of the supersonic flutter capability, an assessment of the harmonic gradient method by Chen and Liu,[2] which is available commercially as ZONA51C,[9] was made and the results were compared with those using the supersonic parallelogram integration program (SPIP).[8] A number of case studies using the Canadian Forces F-18 were carried out, but only the wing results are discussed in this Note because comparisons with the program SPIP can be made only for models having noninterfering simple trapezoidal planforms with supersonic trailing edges.

The first example given herein compares the pressure distributions on the wing surface for rigid-body motion of the aircraft. The second example gives flutter results for the wing using mode shapes computed from NASTRAN.

Aerodynamic Modeling

The planform of the F-18 wing extended to the fuselage centerline is shown in Fig. 1. In using the SPIP computer program, a set of quadrature points is specified on the wing surface; the velocity potentials are then evaluated at these points for each mode shape being analyzed. From the velocity potentials, complex pressure coefficients and generalized forces are computed. Unless otherwise stated, 272 points are used in the computations, the locations of which are indicated in Fig. 1a.

The paneling of the F-18 wing for the ZONA51C computer code is shown in Fig. 1b. For all the computations described in this Note, 126 elements are used.

Mode Shapes

In the first example, the three modes considered are: 1) Wing plunge: $h_w = 100$; 2) Wing unit pitch about one-third local chord: $h_w = (x - 62.68 - 0.318y)$; and 3) Leading-edge flaps unit rotation (inboard and outboard flaps moving in unison): $h_w = 0$ and $\beta = 1$, where h_w is the local perpendicular displacement of the wing surface and β the rotation of the leading-edge flaps about the hinge line. The coordinates of the wing planform are given in Fig. 1a.

In the second example, the mode shapes of the wing are obtained from NASTRAN dynamic normal modes solution routine. The aircraft is defined by a set of finite-element bars, lumped masses, and springs that provide a good analytical approximation to the dynamic behavior of the actual airplane.

Results

Rigid-Modes Pressure Distributions

In addition to the plunge and pitch modes, the leading-edge flap rotation mode is included to demonstrate the effect of varying the number of elements or quadrature points on the aerodynamics of flaps and control surfaces. Figure 2 shows the distributions of the real part of the pressure coefficient ΔC_p for these three modes at 0.048, 0.332, 0.588, 0.794, and 0.965% of the wing span. The Mach number is 1.1 and the reduced frequency k_r based on the semichord is 2.0. This value of k_r is considered high for flutter analysis, but is used in the test case since it places a greater demand on the accuracies of the aerodynamic codes. The pressures match fairly well, but agreement becomes progressively worse as the wing tip is ap-

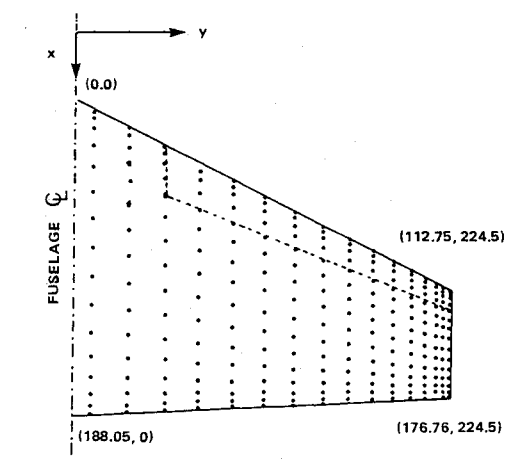

a) SPIP program with 272 quadrature points

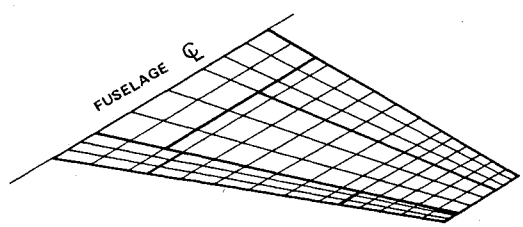

b) ZONA51C program with 126 elements

Fig. 1 Aerodynamic modeling of F-18 wing.

Received April 22, 1988, revision received July 27, 1988.

*Senior Research Officer, High Speed Aerodynamics Laboratory, National Aeronautical Establishment. Member AIAA.

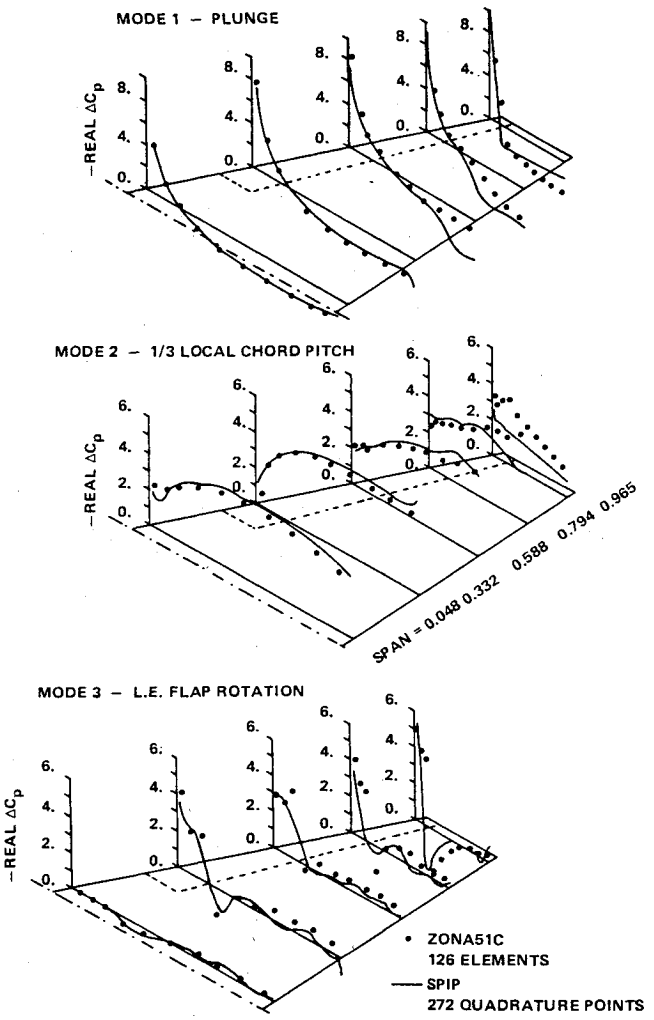

Fig. 2 Distributions of real part of ΔC_p for rigid-body modes.

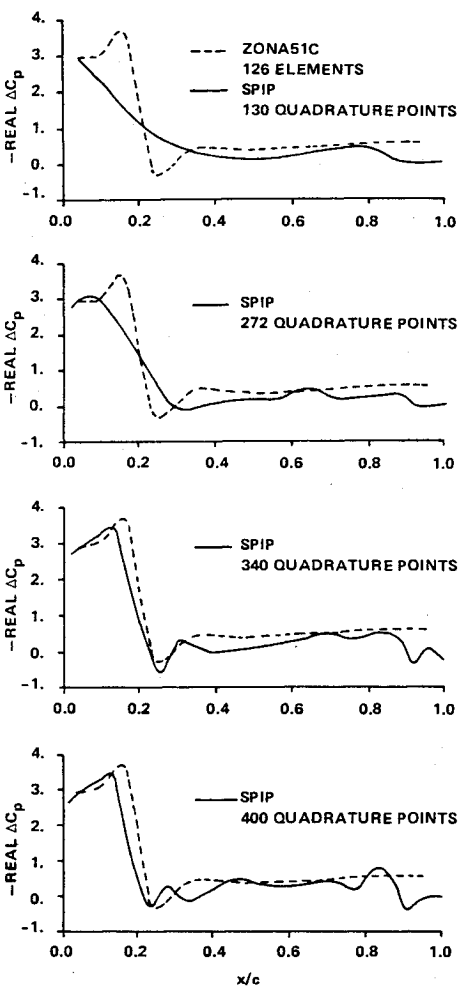

Fig. 3 Effect of number of quadrature points on pressure distributions at 0.588 span, $M = 1.1$, and $k_r = 2$.

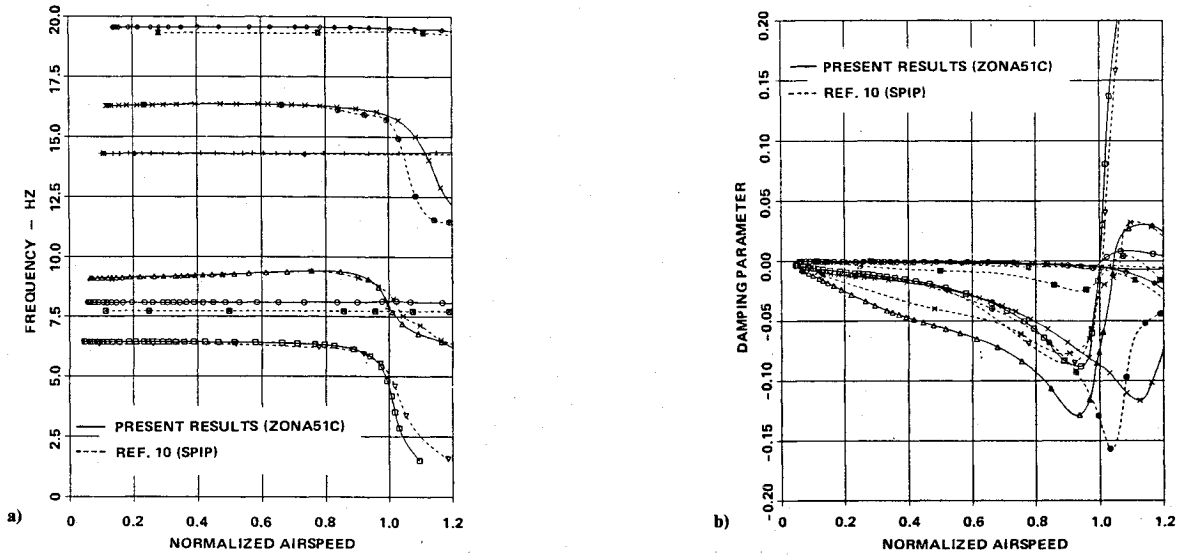

Fig. 4 Frequency and damping plots vs normalized air speed for F-18 test case at sea level and $M = 1.15$.

proached. For small values of k_r, the agreement is found to be extremely good. The same conclusions can be made for the imaginary part of ΔC_p. For the leading-edge flap rotation mode, the finite pressure jump at the hinge line is well predicted by ZONA51C, while the results from SPIP show a gradual change in pressure across the flap onto the wing surface. This is illustrated in Fig. 3, which shows that the SPIP computer code requires a greater number of quadrature points when sharp pressure changes are encountered.

Flutter Analysis of F-18 Wing

For the F-18 wing flutter analysis, the antisymmetric modes are considered in this example and 30 modes are used in the computations. The Mach number is 1.15 and the analysis is carried out at sea level. Figure 4 shows the damping and frequencies for the first few modes using the *V-g* flutter method. The SPIP results are obtained from Ref. 10, but there are no details available on the NASTRAN and aerodynamic modeling. There are some small discrepancies in the modal frequen-

cies compared with present results and it is suspected that the structural data are slightly different. However, the predicted flutter velocities are practically the same and the agreement is better than 0.5%.

Conclusions

The harmonic gradient and the source distribution methods for computing supersonic aerodynamics are compared using the F-18 as a test case. For rigid-body modes, good agreement in pressure distributions is observed except for high reduced frequencies and near the wing tip. For oscillating flaps and control surfaces, the SPIP program requires a large number of source points to give the proper pressure jump across the hinge line, while the ZONA51C code handles the sharp pressure change quite satisfactorily without requiring additional elements to be placed near the hinge line. Flutter results for the F-18 wing agree very well between these two aerodynamic methods.

Acknowledgments

The author wishes to thank the National Defence of Canada for their support and making available some F-18 data.

References

[1]Jones, W. P. and Appa, K., "Unsteady Supersonic Aerodynamic Theory for Interfering Surfaces by the Method of Potential Gradient," NASA CR-2898, 1977.

[2]Chen, P. C. and Liu, D. D., "A Harmonic Gradient Method for Unsteady Supersonic Flow Calculations," *Journal of Aircraft*, Vol. 22, May 1985, pp. 371-379.

[3]Hounjet, M. H. L., "Improved Potential Gradient Method to Calculate Airloads on Oscillating Supersonic Interfering Surfaces," *Journal of Aircraft*, Vol. 19, May 1982, pp. 390-399.

[4]Zartarian, G. and Hsu, P. T., "Theoretical Studies on the Prediction on Unsteady Airloads on Elastic Wings," WADC TR56-97, Dec. 1955.

[5]Ii, J. M., Borland, C. J., and Hogley, J. R., "Prediction of Unsteady Aerodynamic Loading of Non-Planar Wings and Wing-Tail Configurations in Supersonic Flows," Air Force Flight Dynamics Lab, TR-71-108, 1972.

[6]Garcia-Fogeda, P. and Liu, D. D., "A Harmonic Potential Panel Method for Flexible Bodies in Unsteady Supersonic Flow," AIAA Paper 86-0007, Jan. 1986.

[7]Rodden, W. P., Giesing, J. P., and Kalman, T. P., "New Developments and Applications of the Subsonic Doublet-Lattice Method for Nonplanar Configurations," *Symposium on Unsteady Aerodynamics for Aeroelastic Analyses of Interfering Surfaces*, AGARD CP 80, May 1970, Paper 4.

[8]Burkhart, T. H., "Numerical Application of Evvard's Supersonic Wing Theory to Flutter Analysis," AIAA Paper 80-0741, 1980.

[9]"Documentation of ZONA51 Code," Zona Technology, Inc., Rept. ZONA 85-1, July 1985.

[10]Potter, M., National Defence of Canada, Ottawa, Canada. Private communication, 1986.

Calculated and Experimental Stresses in Solid and Ring Slot Parachutes

William L. Garrard* and Michael L. Konicke†
University of Minnesota, Minneapolis, Minnesota

Introduction

IN the late 1960's and early 1970's Mullins and co-workers[1-3] developed a finite-element code called CANO (canopy stress analysis) to calculate the canopy shape, stresses in the horizontal ribbons, and forces in the radial members and suspension lines for ribbon parachutes. Recently, Garrard and co-workers[4-6] developed modified versions of CANO and compared the stresses and shapes calculated using these codes with experimental results for ribbon parachutes. Also, Sundberg[7] developed a new parachute stress analysis code called CALA (canopy loads analysis) that has many assumptions in common with CANO but exhibits better convergence reliability.

CANO has become the standard code for parachute stress analysis and has been used to design a variety of high-performance ribbon parchutes[8] and, more recently, solid parachutes.[9] However, one of the basic assumptions underlying both CANO and CALA is that the canopy is under uniaxial stress in the circumferential direction. This is a good assumption for ribbon parachutes but not for solid or ring-slot parachutes. Garrard and co-workers[10-12] measured stresses in both solid and simulated ring-slot parachutes, and the purpose of this Note is to compare these measured results with those obtained using various versions of CANO. To the authors' knowledge, such comparisons have not been reported. CANO and CALA have been shown to yield similar numerical results when applied to the same parachute; therefore, comparisons between CALA and the experimental results should be about the same as for CANO.

CANO requires as inputs 1) the uninflated canopy geometry, 2) the material force/deformation relationships for all canopy elements, 3) the axial load on the canopy, and 4) an estimate of the pressure distribution on the canopy. Outputs of CANO are canopy shape and forces and stresses in canopy elements. CANO begins its solution at the skirt and iteratively solves algebraic equilibrium and force/deformations relations from the skirt to the vent, trying to match two boundary conditions (one somewhat arbitrary) at the vent. CANO iteratively varies two parameters, skirt radius and magnitude of the differential pressure disibution curve, to try and converge to a solution. Since CANO starts at the skirt and tries to match a boundary condition at the vent, errors in shape at the vent can sometimes lead to errors in structural loading or convergence problems.

The solution method of CANO is as follows. The axial components of the suspension line loads balance the axial force input. Suspension line loads are determined by an iterative solution of the equilibrium and force/deformation equations for the suspension lines. Once suspension line loads have been determined, computations on the canopy proceed from the skirt to the vent. The pressure on a horizontal element is balanced by the hoop stress on the ends of this element. This hoop stress is, in turn, in equilibrium with the loads in the radial elements connected to the ends of the horizontal element. The suspension lines comprise the elements attached to the lower side of the horizontal element at the skirt. The loads in the suspension lines are known as they were calculated previously to balance the axial load. The loads and geometry of the skirt horizontal element and the radials attached to the upper side of this element are then calculated using equilibrium and compatibility between the stretched and geometrically determined length of the horizontal element. These form a coupled set of nonlinear algebraic equations that must be solved numerically. The skirt radius is iteratively adjusted until equilibrium and geometric compatibility are achieved. Then, the calculations proceed to the next horizontal element. The forces in the radials attached to the lower side of the horizontal are known from the calculations performed on the previous element, and the geometry and forces in the horizontal and the radial elements attached to its upper side are determined in the same manner as for the skirt horizontal. Calculations proceed sequentially to the vent.

Once the vent is reached, the force due to the pressure on the vent hole is calculated. If the calculated axial force component due to the radials converging at the vent is not between 25

Presented in part as Paper 86-2488 at the AIAA 9th Aerodynamic Decelerator and Balloon Technology Conference, Albuquerque, NM, Oct. 7-9, 1986; received Oct. 1, 1987; revision received April 1,1988.

*Professor, Department of Aerospace Engineering and Mechanics. Associate Fellow AIAA.

†Research Assistant, Department of Aerospace Engineering and Mechanics; currently Engineer, Boeing Commerical Airplane Co., Seattle WA. Member AIAA.